

## Sense of shear and displacement estimates in the Abeibara–Rarhous late Pan-African shear zone, Adrar des Iforas, Mali

ANNE-MARIE BOULLIER

Centre de Recherches Pétrographiques et Géochimiques, BP 20 F54501, Vandoeuvre-les-Nancy Cedex, France

(Received 31 January 1984; accepted in revised form 5 April 1985)

**Abstract**—The late Pan-African Abeibara–Rarhous shear zone in the Adrar des Iforas (Mali) is described and studied with the aim of defining the direction, sense of movement and amount of displacement along the zone. It is a strike-slip shear zone, the dextral sense of which is demonstrated at the scale of the map by the rotation of the related mylonitic foliation and at the scale of the thin section with characteristic microstructures. Preferred orientation of quartz *c*-axes is tentatively used; three quartz-rich samples of 35% or more quartz indicate dextral strike-slip movement, but other samples do not show preferred orientation of quartz *c*-axes. Strain measurements have been performed on one half of the shear zone using established techniques and a new technique using the thickness of mylonitic layering. The results vary along the length of the shear zone when using the same method and for the same cross-section when using the three methods together. A mean value of 4 km is obtained for total displacement which is low when considering the apparent width of the shear zone. This result is discussed in view of the assumptions involved in the strain estimation. The tectonic history of the Abeibara–Rarhous shear zone and its significance in the Trans-Saharan Pan-African collisional belt are discussed.

**Résumé**—La zone de cisaillement tardi-Pan-Africaine de Abeibara–Rarhous dans l'Adrar des Iforas (Mali), est décrite et étudiée dans le but de définir la direction et le sens du mouvement ainsi que le déplacement le long de cette zone de déformation ductile. C'est un décrochement dextre dont le sens est démontré par la rotation de la foliation mylonitique associée et des structures planaires antérieures. L'orientation préférentielle des axes *c* du quartz est aussi utilisée, mais à l'exception de trois échantillons relativement riches en quartz (35% ou plus) qui confirment le sens de décrochement dextre, les autres échantillons ne montrent pas d'orientation préférentielle forte de réseau. Des mesures de déformation finie ont été faites sur une moitié de la zone de cisaillement, en appliquant les techniques établies et une nouvelle technique utilisant l'épaisseur de rubanement mylonitique. Les résultats varient le long de la zone de cisaillement quand on utilise une seule méthode, et sur une même coupe quand on utilise les trois méthodes à la fois. La valeur minimale moyenne obtenue pour le déplacement total (4 km) semble faible si on considère la largeur apparente de la zone de cisaillement. Ce résultat est discuté en fonction des restrictions faites pour l'utilisation des méthodes d'estimation de la déformation finie, de l'histoire tectonique de cette zone de cisaillement de Abeibara–Rarhous, et de sa signification dans la chaîne de collision Pan-Africaine Trans-Saharienne.

### INTRODUCTION

THE PAN-AFRICAN Trans-Saharan belt (Cahen & Snelling 1984) is the result of the collision between the West African Craton and the Pan-African mobile belt (Fig. 1) which occurred about 600 Ma ago (Bertrand & Caby 1978, Black *et al.* 1979). The latest stage of the collision is characterized by large N–S faults and shear zones that have been recognized for a long time as major structures of the Hoggar Shield by Lelubre (1952) and Caby (1968) and that have been considered to approximate slip lines (Caby *et al.* 1981, Lesquer & Louis 1982) similar to those observed in Eurasia by Molnar & Tapponnier (1975). This paper deals with the Abeibara–Rarhous shear zone, one of the shear zones in the central part of the Adrar des Iforas. It appears very clearly on satellite and aerial photographs and is the widest (6–7 km) known shear zone in the Adrar des Iforas, but no marker allows us to determine the displacement along it directly. However, a strain gradient exists in its eastern part, in the Eburnean granulites, that enables one to determine the direction, the sense, and the minimum amplitude of the movement using field observations, microstructures, preferred orientations of quartz *c*-axes, and different techniques of strain estimation. With these results at hand, it should then be possible to integrate this shear

zone in a regional context, to compare it with other faults and shear zones in the Hoggar Shield, and to discuss the collision model proposed by Caby *et al.* (1981) for the Trans-Saharan Pan-African belt (Cahen & Snelling 1984).

### GENERAL GEOLOGICAL SETTING

In the central Adrar des Iforas, three main Pan-African phases of deformation have been identified (Wright 1979, Boullier 1979, Davison 1980). The first phase  $D_1$  corresponds to a deformation during which the granulitic Eburnean basement (the Iforas granulitic unit) and its Upper Proterozoic cover have been thrust northwards over a high grade gneissic unit, the so-called Kidalian Assemblage (Boullier *et al.* 1978). The mylonitic base of the Iforas granulitic unit is preserved on its northern and south-eastern borders. A flat-lying foliation, occasional, recumbent sheath folds, and a North–South stretching lineation are developed in the Kidalian Assemblage during  $D_1$ . This deformation phase is not precisely dated but is placed at before 696 Ma by Caby *et al.* (1981) and Bertrand & Davison (1981) and between 696 and 613 Ma by Ball & Caby (1985).

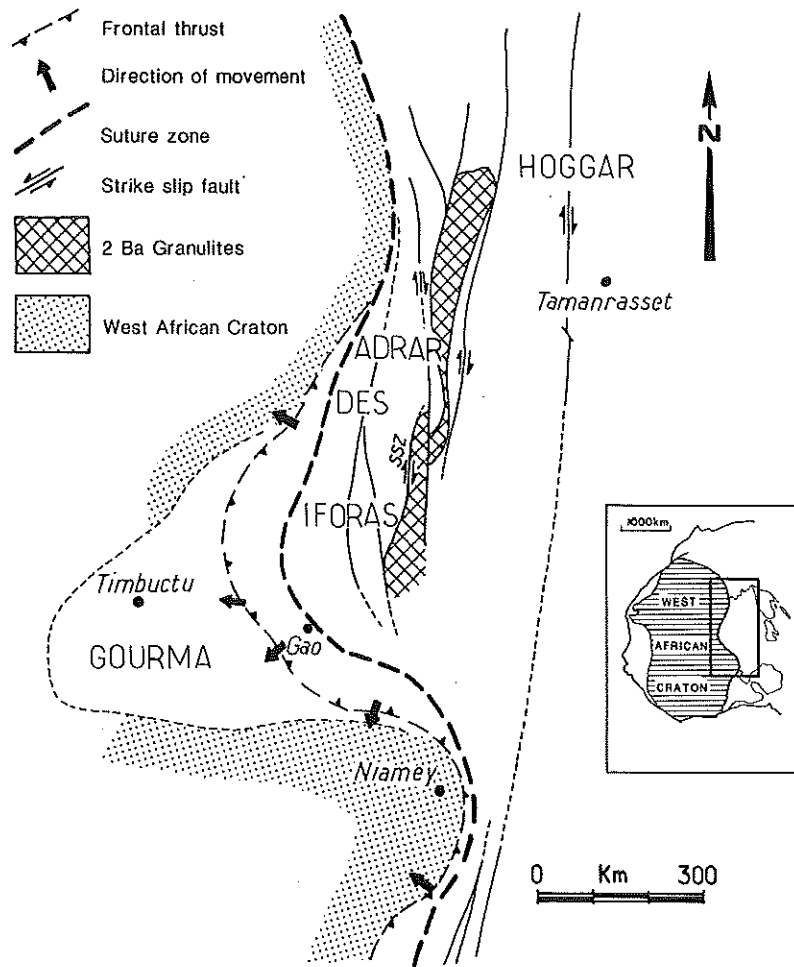


Fig. 1. Locality map of the Pan-African collisional belt of the Adrar des Iforas (Mali) along the eastern margin of the West African Craton. The suture zone is drawn as defined by gravimetric anomalies (Bayer & Lesquer 1978). SSZ: studied Late Pan-African shear zone along the western margin of the Iforas Eburnean (2000 Ma) granulitic unit.

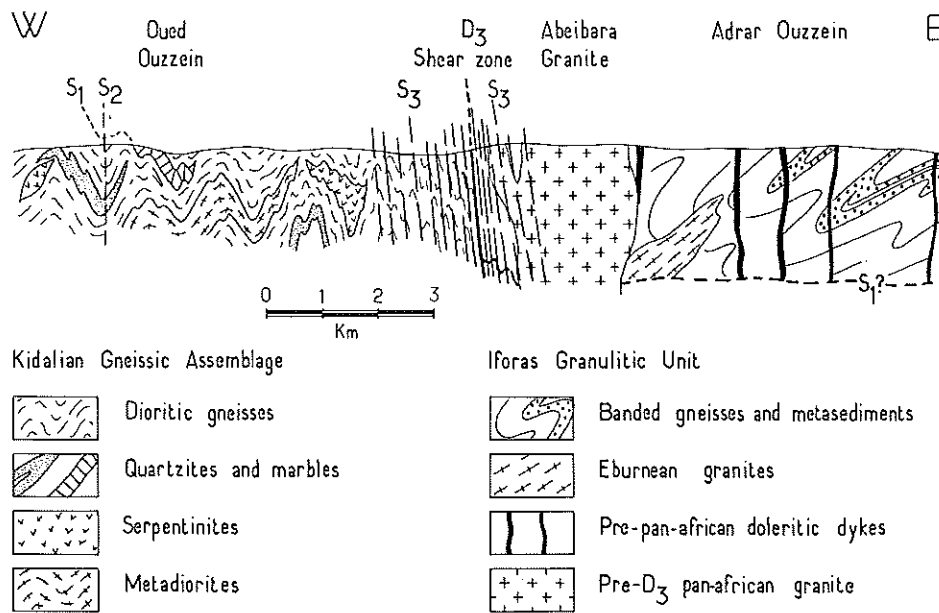


Fig. 2. Schematic section across the Abeibara-Rarhous shear zone along the western margin of the Iforas granulitic unit which is interpreted as a  $D_1$  nappe lying upon the Kidalian gneissic assemblage.  $D_1$ ,  $D_2$  and  $D_3$  structures are superimposed within the Kidalian gneissic assemblage. In the Iforas granulitic unit only  $S_3$  is visible on the western margin.

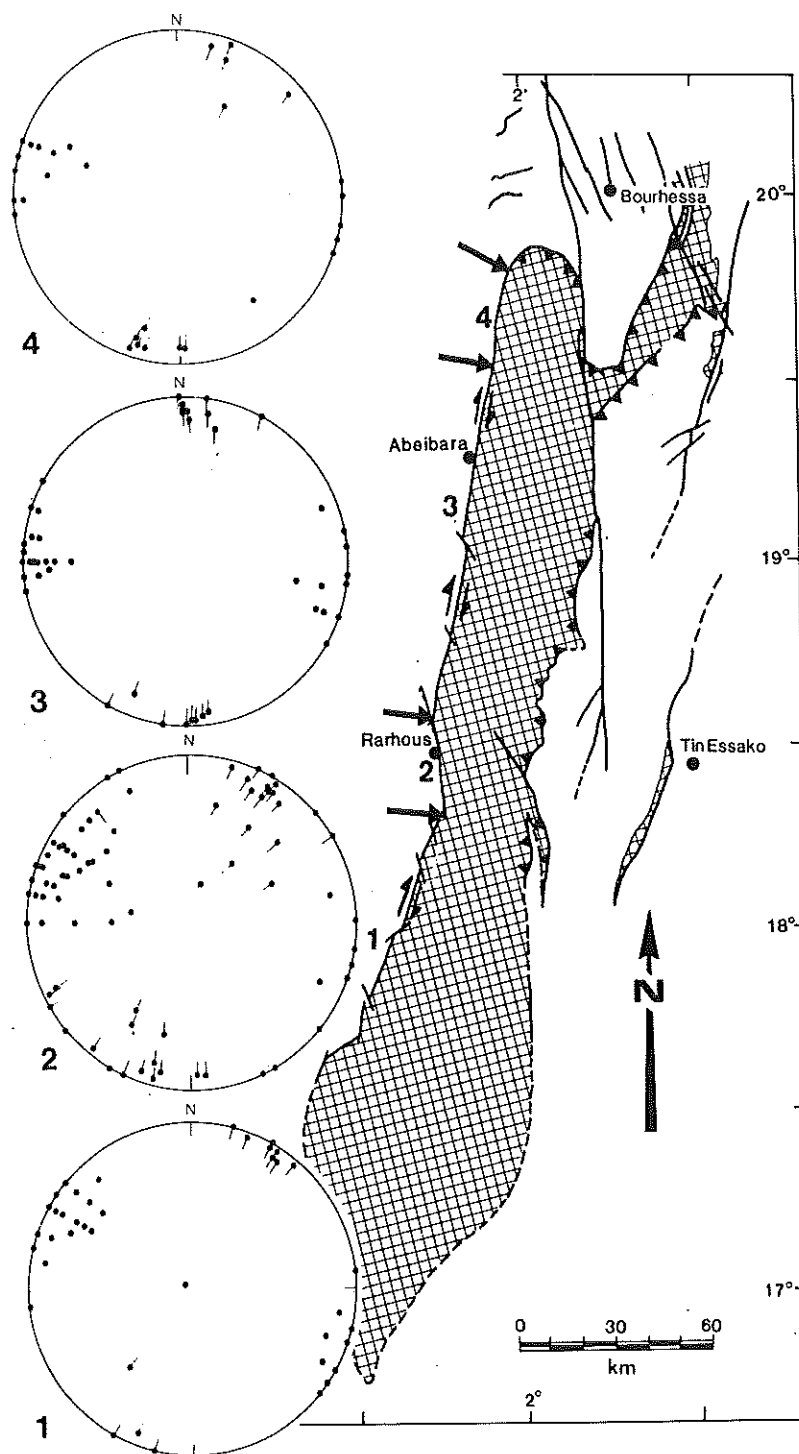


Fig. 3. Stereographic projection (lower hemisphere) of the poles to  $S_3$  mylonitic foliation (points) and  $L_3$  stretching lineations (dots with tails) along the Abeibara–Rarhous  $D_3$  shear zone on the western margin of the Iforas granulitic unit. Except in area 2, which has been disturbed by a later sinistral NNW–SSE fault,  $S_3$  foliations are vertical, striking N-10° to N-20° and bear a horizontal  $L_3$  lineation.

The  $D_2$  phase corresponds to a SSE–NNW and then an ESE–WNW compression (Wright 1979, Boullier 1982) expressed by ENE–WSW to NNE–SSW upright to overturned isoclinal folds. The Eburnean granulites ( $D_1$  nappe) constitute the core of a large  $D_2$  synform. This  $D_2$  phase is well dated at around 610–600 Ma (Bertrand *et al.* 1985).

The  $D_3$  phase corresponds to N–S to N-20° trending strike-slip shear zones and faults described by Wright (1979), Boullier (1980, 1982) and Davison (1980). The Abeibara–Rarhous shear zone is one of these  $D_3$  shear zones. U–Pb and  $^{39}\text{Ar}/^{40}\text{Ar}$  geochronological dating indicate that it was active between 566 and 535 Ma (Lancelot *et al.* 1983) and confirms its late Pan-African age.

## DESCRIPTION OF THE ABEIBARA-RARHOUS SHEAR ZONE

The Abeibara-Rarhous shear zone trends N-10° and separates two geologically different blocks (Fig. 2). On the west block, the gneissic Kidalian Assemblage has suffered the three Pan-African deformation phases described above ( $D_1$ ,  $D_2$ ,  $D_3$ ). Far away from the shear zone, the  $S_1$  subhorizontal foliation bears a N-S to N-10° stretching lineation and is folded by NNE-SSW  $D_2$  folds. Both deformations were accomplished at amphibolite facies conditions. The N-10°  $S_3$  vertical foliation is almost subparallel to  $S_2$ , but corresponds to lower metamorphic conditions of upper amphibolite facies to greenschist facies;  $S_3$  bears a horizontal N-10° stretching lineation. Thus  $S_1$ ,  $S_2$  and  $S_3$  are subparallel to the shear zone in a band 5-6 km wide. Consequently, it is not possible by observing the structures west of the shear zone to determine how much strain should be attributed to  $D_1$ ,  $D_2$  or to  $D_3$  individually, because the three deformation phases are almost homoaxial.

On the east block, the Iforas granulitic unit is mainly composed of a homogeneous banded formation of quartzo-feldspathic subalkaline gneisses metamorphosed under granulitic facies conditions during the Eburnean period (2400-2100 Ma, Lancelot *et al.* 1983). Except in the north,  $D_3$  is the only Pan-African deformation phase observed in the Iforas granulitic unit along the Abeibara-Rarhous shear zone. It is characterized by a strain gradient in a zone 500-1500 m wide and by a vertical N-350° to N-10° foliation with a horizontal stretching lineation (Fig. 3).

As the lithologies and the pre- $D_3$  tectonic history of the western polyphase gneisses are complex, the deformation features related to the  $D_3$  Abeibara-Rarhous shear zone have been mainly studied in the mylonitized granulites. The L-S tectonites within the shear zone suggest that the deformation was plane strain and the horizontal stretching lineation is assumed to be close to the movement direction. Consequently, the Abeibara-Rarhous structure is a strike-slip shear zone, the sense of which will now be determined.

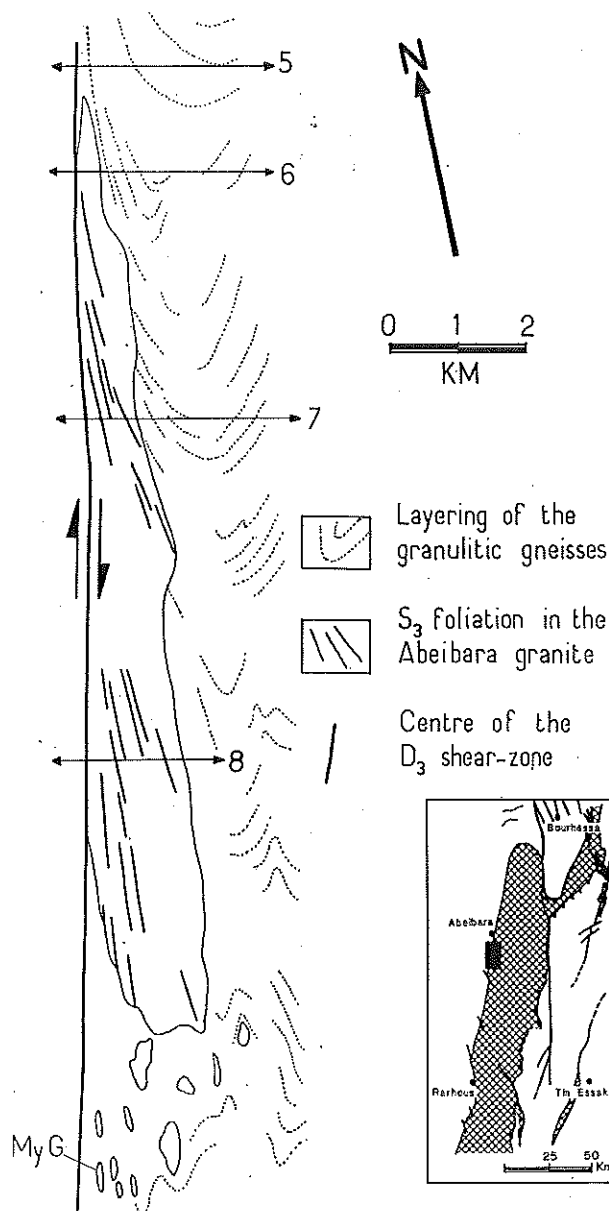


Fig. 4. Schematic map of the Pan-African pre- $D_3$  Abeibara granite showing the rotation of the  $S_3$  mylonitic foliation and of the granulitic layering towards the centre of the shear zone (map drawn from the aerial photographs NE 31 XX and 351). The numbers refer to the sections along which strain measurements have been made.

## DETERMINATION OF THE SENSE OF SHEAR

### Field observations

Observations on the 1/50,000 aerial photographs and on the outcrop of the pre- $D_3$  Pan-African Abeibara granite show that the  $S_3$  mylonitic foliation is deflected into the shear zone, indicating a dextral sense of shear (Fig. 4). The granulitic layering of the banded gneisses is similarly deflected (Fig. 5). At its northern termination, the Abeibara-Rarhous shear zone divides into several dextral strike slip faults which curve towards the penecontemporaneous dextral strike slip Andjour-Tamaradant fault (Fig. 6). The displacement of the north-eastern limit of the Iforas granulitic unit (see Fig. 3) indicates a movement of 28 km along this fault. Some

NE-SW adamellitic dykes and E-W sinistral faults, the type B secondary faults of Chinnery (1966), could be a response to the same stress field as that which caused the  $D_3$  Abeibara-Rarhous shear zone.

### Microstructures

The evolution of the microstructures in the Abeibara-Rarhous shear zone has already been described (Boullier 1980). All stages are observed from protomylonites to ultramylonites, the increase in the deformation being accompanied by a decrease in the grain size due to different plastic and cataclastic behaviour of the constituent minerals.

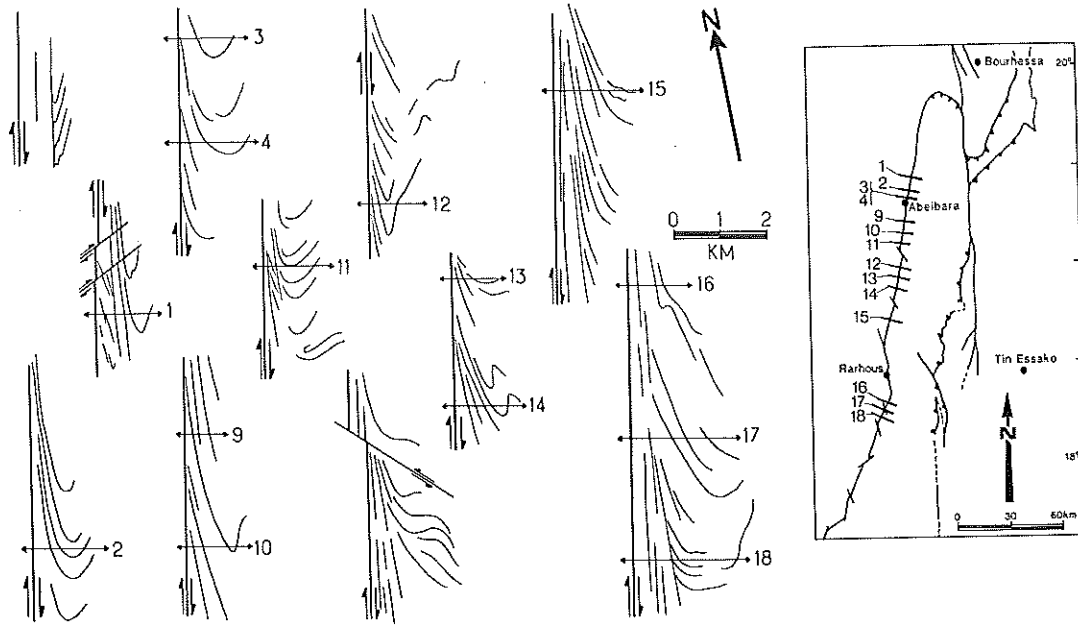


Fig. 5. Maps drawn after aerial photographs (NE 31 XX and XIV) to show rotation of the granulitic layering towards the centre of the Abeibara-Rarhous shear zone. Numbers refer to sections from north to south along which strain measurements have been made (see locality map).

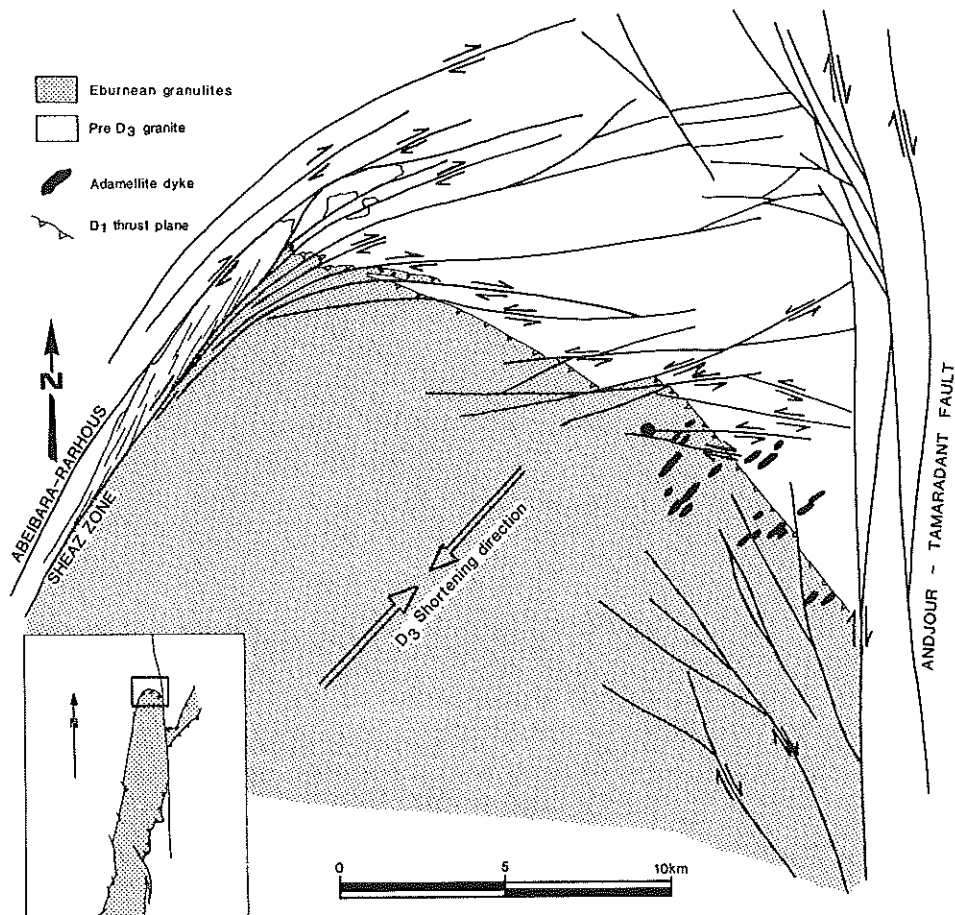


Fig. 6. Map of the northern part of the Iforas granulitic unit, where the Abeibara-Rarhous shear zone curves towards the Andjour-Tamaradant dextral fault. Note the pre- $D_3$  granite and the limit of the granulites which are deformed by the shear zone. The  $D_3$  shortening direction is deduced from the orientation of N-S to N-20° dextral faults, E-W sinistral faults and NE-SW adamellitic dykes.

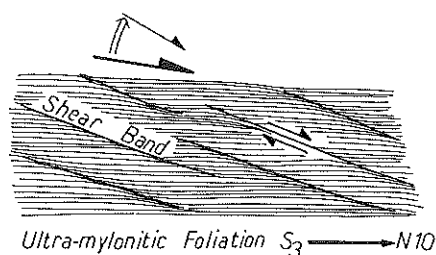


Fig. 7. Shear bands superimposed on the vertical mylonitic foliation  $S_3$ . The relative orientation of both planes is constant all along the Abeibara–Rarhous shear zone and indicates a dextral sense of shear.

$S_3$  is defined by a greenschist facies metamorphic assemblage and by mylonitic layering in the form of an alternation of dark layers of green biotite, opaque phases and accessory minerals, and light layers of albite, microcline and/or polycrystalline quartz ribbons, the latter being of type II-2 of Boullier & Bouchez (1978). However, in the centre of the shear zone, grain size is very small ( $20 \mu\text{m}$ ), mineral phases are mixed, and the mylonitic banding tends to disappear.

At thin section scale, the best shear sense criteria are the vertical ductile shear bands as defined by Gapais & White (1982) or  $C'$  planes (Berthé *et al.* 1979) or  $C$  planes (extended terminology of Lister & Snoke 1984), which are superimposed on the  $S_3$  mylonitic foliation with a consistent geometry indicating a dextral shearing (Fig. 7). They only appear in the centre of the shear zone where the well-developed  $S_3$  foliation ( $XY$  plane) is subparallel to the shear zone boundary; they are low-strain shear bands with an orientation strongly divergent from that of the bulk shear plane ( $N-30^\circ$  vs  $N-10^\circ$ ), but they are characterized by the same green biotite as  $S_3$ . These oblique structures could be explained as a response of the anisotropy to stretching in a continuous deformation, thus being examples of the extensional cleavage of Platt & Vissers (1980) or fig. 19(a) of Lister & Snoke (1984); but if that were the case, both antithetic and synthetic shear planes should be seen. Only dextral shear bands exist in the Abeibara–Rarhous shear zone, so it is suggested that these oblique structures involve a small rotation of the regional shortening direction toward a roughly E–W direction. This rotation will be discussed later when the regional tectonic history of the Adrar des Iforas is considered.

#### Quartz $c$ -axis preferred orientations

Quartz  $c$ -axis preferred orientations have been studied optically in several samples along an E–W cross-section (Fig. 8). Most samples do not show strong preferred lattice orientation. Some diagrams show a pole-free area around the stretching lineation  $X$  (My7C, My9) or near the  $XZ$  plane (My8), but they can almost be interpreted in terms of a random  $c$ -axis orientation. This random orientation has been confirmed with X-ray goniometric study at the University of Leeds for  $[10\bar{1}0]$  and  $[10\bar{2}0]$  in three ultramylonites (My7B, My7C and My6A) in which the grain size was too small to permit optical investigation.

Nevertheless, four samples (My2, MyG, IB761 and IB765) show a  $c$ -axis preferred orientation defined by a single girdle in which a maximum occurs near  $Z$  (My2) or near  $Y$  (IB765). Except in sample MyG, this girdle is clearly oblique to the strain axes. In the case of MyG, the measurements have been plotted separately for porphyroclasts and small equant new grains, but the  $c$ -axis preferred orientation is almost the same in both cases. This result is similar to those obtained by Hobbs (1968), Wilson (1973), Marjoribanks (1976), Bouchez (1977) and Garcia Celma (1982).

The interpretation of the observed preferred lattice orientations for this shear zone is that the intensity of preferred orientation is related not to strain (Burg & Laurent 1978, Berthé *et al.* 1979) but to the percentage of quartz in the rocks (Starkey & Cutforth 1978). In the present case, the rocks that present a well-defined preferred quartz lattice orientation are those with at least 35% quartz.

The intensity of preferred lattice orientation also appears to be related to the mechanism of deformation. Intracrystalline gliding on specific slip systems gives rise to preferred orientation (Nicolas *et al.* 1973). According to different mathematical models, the elements of an emerging pattern are usually evident only after about 30% shortening (Lister & Hobbs 1980, Etchecopar 1977). If the grain size is small enough, the deformation mechanism can change from intracrystalline glide to grain boundary sliding (Boullier & Gueguen 1975, White 1976); consequently, the lattice-preferred orientation achieved in the first stages of mylonitization could be progressively obliterated at higher strains (Ashby & Verrall 1973). That may well have happened in the ultramylonites studied here; the fine average grain size of about  $20 \mu\text{m}$  and the presence of different mineral phases may have prevented recrystallization and promoted grain boundary sliding.

In cases where lattice-preferred orientation is clearly defined, assuming that the stretching lineation is close to the transport direction, the  $c$ -axis girdle indicates intracrystalline slip in the  $\langle a \rangle$  crystallographic direction (Bouchez *et al.* 1979, Bouchez & Pécher 1981, Schmid *et al.* 1981). The various positions of maxima in the girdle of  $c$ -axes correspond to two or three glide systems that may be operative in the samples (Bouchez & Pécher 1981). In the case of the Abeibara–Rarhous shear zone, the orientation of  $[10\bar{1}0]$  is not known and the interpretation of the  $c$ -axis girdle is based on the comparison with similar patterns cited above: the  $X$  maximum (My2) would correspond to predominantly basal slip (0001) in the  $\langle a \rangle$  crystallographic direction and the  $Y$  maximum to predominantly prismatic slip in the same direction.

The fact that the  $c$ -axis girdle is asymmetric and oblique to the foliation suggests that the deformation occurred under conditions close to those of plane strain (Bouchez *et al.* 1983, Simpson & Schmid 1983 and Lister & Snoke 1984), and one can deduce the sense of shear from the asymmetry: it is dextral in the case of the Abeibara–Rarhous shear zone and consistent with field observations.

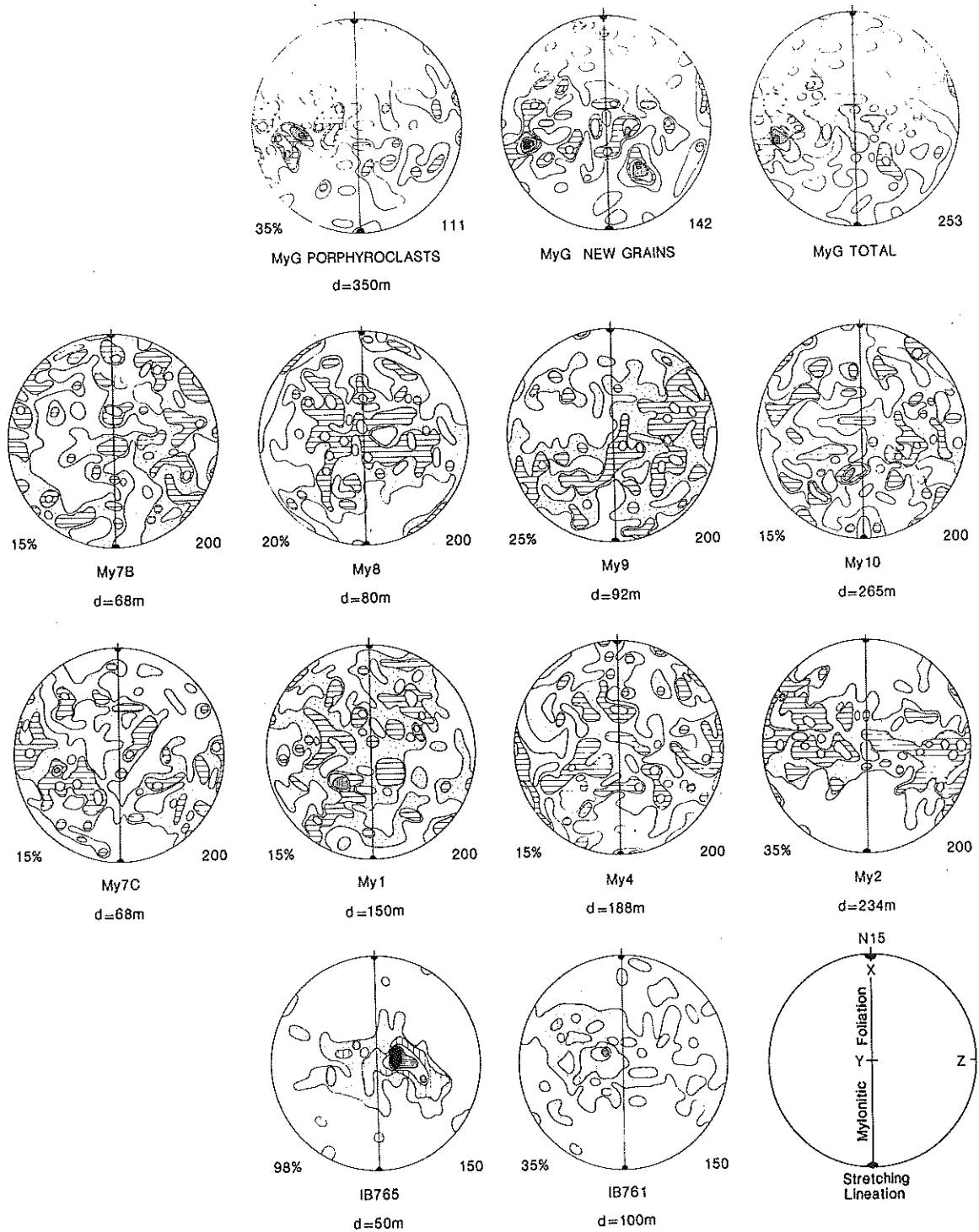


Fig. 8. Preferred lattice orientations of quartz *c*-axes in mylonites (lower hemisphere). The percentage of quartz, the number of measurements and the distance (*d*) from the centre of the shear zone are given for each sample. The contours are at 1, 3, 5, 7, 9 and 11% points per 1/220 surface area of the sphere (Bouchez & Mercier 1974). The orientation is the same for all the samples, the projection plane being nearly horizontal. The *S*<sub>3</sub> mylonitic foliation is vertical at N-15° and *X* is the horizontal stretching lineation. MyG is a mylonitic granite (pre-*D*<sub>3</sub> Abeibara granite) located on Fig. 4. My7B, My7C, My8, My9 and My10 correspond to section 11 and My1, My4 and My2 to section 10. The samples IB765 and IB761 were taken on profile 16 (see Fig. 5 for the localities of the profiles).

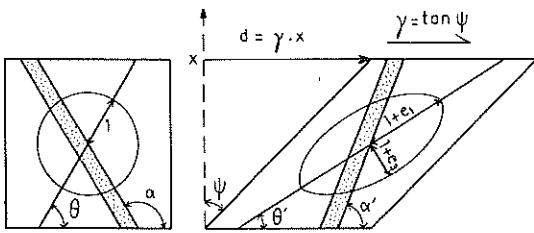


Fig. 9. Relation of the strain ellipse to shear in a simple shear system with no volume change (Ramsay 1980).

### Conclusion on the sense of shear

The sense of shear has been clearly established using both field structures and microstructures to be dextral. Using *c*-axis preferred orientation alone, it would have been difficult to affirm an unambiguous dextral sense of shear since only a few of the studied samples show a clear *c*-axis pattern. My observations confirm Simpson & Schmid's (1983) conclusions concerning reliable structures for the determination of sense of shear in regions where no displaced marker horizon can be found.

### STRAIN ESTIMATION

Knowing that the Abeibara–Rarhous shear zone is a dextral strike-slip vertical shear zone, it is now useful to determine the amount of displacement along it. The methods of strain measurement applied to estimate the shear strain are based on three assumptions:

(1) The deformation is plane strain and due to shearing only. This assumption is based on the *L*–*S* fabric of the tectonites (strong lineation but no apparent constriction) and on the characteristics of the deformation at the map, thin section, and lattice scales, suggesting rotation and plane strain. But the lack of strain markers means that this is an approximation, to be kept in mind until discussion of the results.

(2) The deformation is presumed to have been at constant volume. The density and composition of the rocks do not show any significant variation across the shear zone (Boullier 1982), so this assumption therefore appears valid.

(3) The deformation is ductile and homogeneous, with no discontinuities across the shear zone. This assumption can be verified at the scale of the sample and at the scale of the outcrop. Except in the centre of the shear zone where cataclasis is often superimposed on the ductile deformation, no important fault has been detected. It must be noted that some highly deformed zones less than 10 m wide could have been missed due to the presence of rivers and superficial cover, and that the value of total displacement could thus have been underestimated.

Because the western part of the Abeibara–Rarhous shear zone is complex and  $S_1$ ,  $S_2$  and  $S_3$  there are parallel and no rotation of any structure is observed, only the

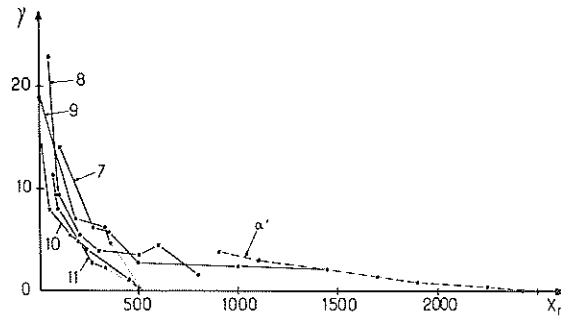


Fig. 10. Graph of the variation in shear strain ( $\gamma$ ) across five cross sections of the  $D_3$  shear zone; the numbers refer to the sections on Figs. 4 and 5.  $\gamma$  has been measured using the orientation of the  $S_3$  foliation ( $\theta'$ ) with respect to the shear zone boundary (first method).

eastern half of the shear zone has been investigated for strain measurement. It will be assumed that the displacement calculated with the three methods is half the total displacement  $D$ .

#### First method: rotation of the $S_3$ foliation

In the case of homogeneous shear (Fig. 9), the angle  $\theta'$  between the  $XY$  flattening plane and the shear plane is related to the shear strain  $\gamma$  by the formula:

$$\tan 2\theta' = 2/\gamma$$

(Ramsay & Graham 1970, equation 36).

If  $x$  is the width of the shear zone, the displacement  $d$  is

$$d = x\gamma.$$

The total displacement  $D$  across a zone of heterogeneous shear strain is

$$D = \int_0^x \gamma dx$$

(Ramsay & Graham 1970, equation 39).

$\theta'$  has been measured in the field for two sections across the eastern part of the shear zone and on aerial photographs for three others (Fig. 10).  $S_3$  is very difficult to see on aerial photographs when it is superimposed on the granulitic layering, but it is clearly visible where it affects the pre- $D_3$  Abeibara granite (Fig. 4). Using this method, five values of  $D/2$  have been obtained (Table 1).

#### Second method: rotation of the Eburnean granulitic layering

The angle  $\alpha'$  between the pre-existing Eburnean granulitic layering and the shear plane (Fig. 9) is related to the shear strain by the formula:

$$\cot \alpha' = \cot \alpha + \gamma$$

(Ramsay 1967, equation 3.71),

where  $\alpha$  is the initial angle between the layering and the shear plane. The displacement is then calculated as in the first method. Measurements of  $\alpha'$  have been made all along the shear zone on aerial photographs only (Figs. 5 and 11). The angle  $\alpha$  is not constant all along the Abeibara–Rarhous shear zone (Fig. 5); consequently,



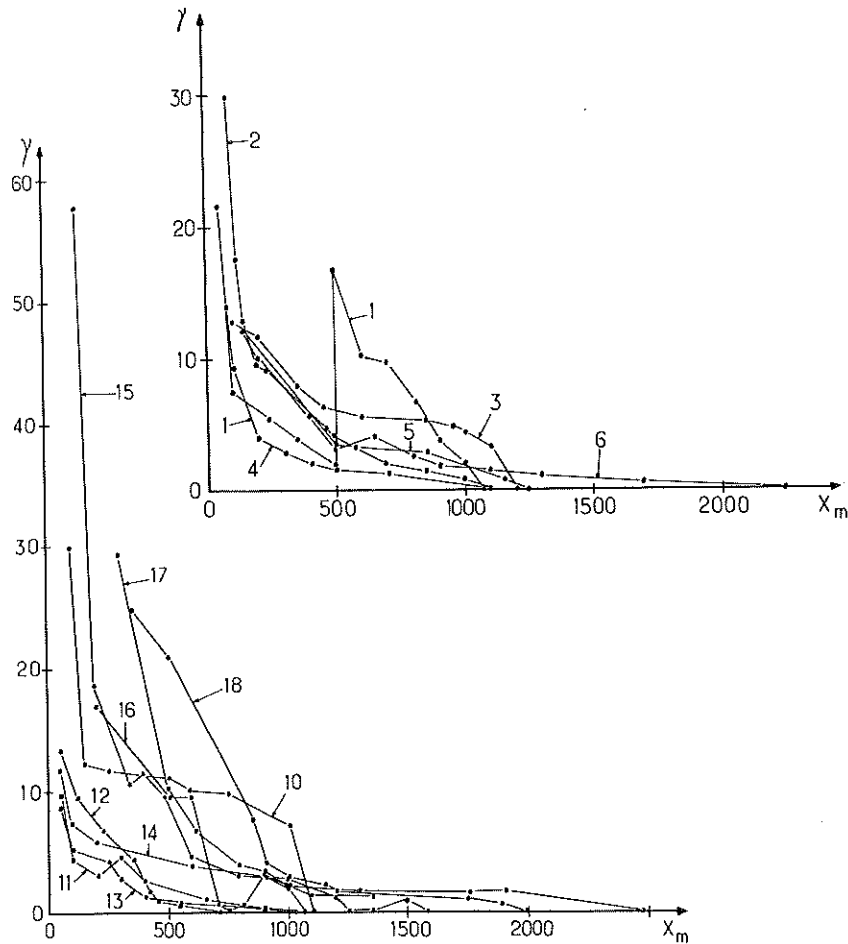


Fig. 11. Graph of the variation in shear strain ( $\gamma$ ) across the  $D_3$  shear zone; the numbers refer to the sections on Figs. 4 and 5.  $\gamma$  has been measured using the orientation of the granulitic layering ( $\alpha'$ ) with respect to the shear zone boundary (second method).

for each cross-section,  $\alpha$  has been taken as the highest value of  $\alpha'$  measured in the anticlockwise sense, from the shear zone to the layering, at the position just where the layering appears to be turned towards the shear plane. Generally, this corresponds to a distance of 2000–

2500 m from the centre of the shear zone.

The results are given in Table 1 and Fig. 11. One set of measurements has been made along a section across the Abeibara granite and its surrounding rocks using the first and second methods together.

Table 1. Displacement along the  $D_3$  shear zone, calculated from strain measurements by three different methods. The stars indicate a cross-section on which two different methods have been used on two different segments

Aerial photograph no.	Section	1st method (Fig. 10)		2nd method (Fig. 11)	3rd method (Fig. 13)
		$\theta'$ aerial photograph $D/2$ (km)	$\theta'$ outcrop $D/2$ (km)	$\alpha'$ aerial photograph $D/2$ (km)	$n/n'$ sample $D/2$ (km)
NE XX 218	1			7.66	
NE XX 274	2			7.76	
NE XX 285	3			8.17	
	4			3.31	
NE XX 340	5			7.07	
	6			7.52	
	7			7.97*	
NE XX 351	8	7.97*			
NE XX 406	9	5.06	3.87		2.36
	10		2.27	11.68	1.97
NE XX 418	11		2.51	2.69	1.89
NE XX 484	12			3.43	
NE XIV 34	13			2.32	
	14			5.08	
NE XIV 148	15			16.98	
NE XIV 370	16			9.85	
	17			16.65	
	18			20.04	

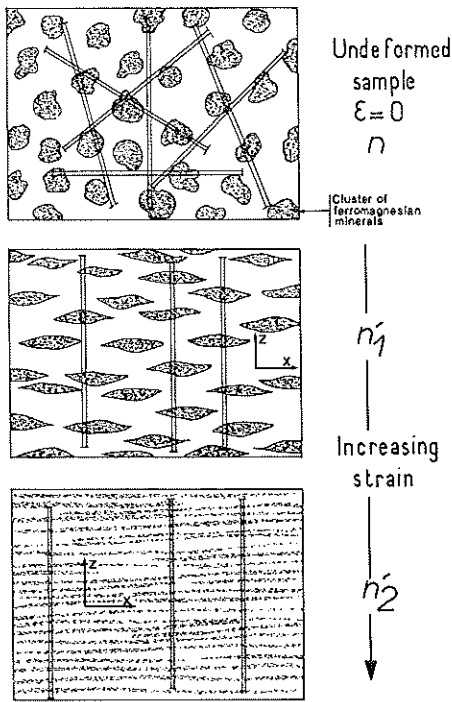


Fig. 12. Method of strain measurement in the Abeibara-Rarhous shear zone using the number of ferromagnesian mineral spots or layers along segments of constant length in the Z direction. The measurements are made on XZ thin sections.  $n/n'$  is a direct estimation of  $\sqrt{\lambda_3}$  or  $(1 + e_3)$ .

#### Third method: thickness of the $S_3$ mylonitic layering

An estimation of the strain has been made petrographically by using the aggregate of biotite and opaque phases resulting from the replacement of clinopyroxene in the granulites. In this method (Fig. 12), the number of biotite clusters is counted in a segment of a constant length  $a$ : the counting is made in different directions for undeformed rocks ( $n$ ) and in the Z direction normal to the  $S_3$  foliation for the mylonites ( $n'$ ). XZ thin sections were used for these measurements. We have

$$n = a/(b_1 + b_2) \quad n' = a/(b'_1 + b'_2),$$

where  $b_1$  and  $b_2$  are the thicknesses of the ferromagnesian and the quartzo-feldspathic layers, respectively. Then

$$n/n' = 1 + e_3 = \sqrt{\lambda_3}.$$

The deformation is assumed to be plane strain; then  $e_2$  is zero and  $\gamma$  can be deduced from  $n/n'$  using the equation

$$\lambda_3 = \frac{\gamma^2 + 2 - \gamma\sqrt{\gamma^2 + 4}}{2} \quad (\text{Ramsay 1967, equation 3.71}).$$

On each cross section,  $\gamma$  is deduced from  $n/n'$  on different samples and  $D/2$  is calculated in the same way as in the two first methods. The results (Fig. 13) are given in Table 1.

#### Discussion of the results

The results vary along the length of the Abeibara-Rarhous shear zone when using the same method, and

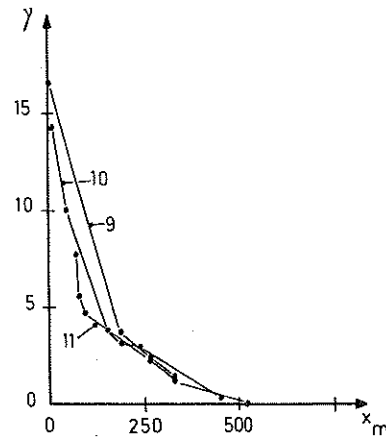


Fig. 13. Graph of the variation in shear strain ( $\gamma$ ) across the Abeibara-Rarhous shear zone using the third method. The numbers refer to the cross-sections on Fig. 5.

for the same cross-section when using the three methods together (Table 1). Actually, keeping in mind the assumptions which have been made for the three methods (see above), each method involves some particular errors and these are addressed in the following remarks.

(1) The centre of the shear zone is well known where it has been recognized in the field (sections 8, 9, 10, 11, 15, 16, 17 and 18). Otherwise, the position of the centre of the shear zone was estimated from aerial photographs. Because contrast between the two sides of the shear zone is not sharp, errors in  $x$  could be up to 100 m at a total apparent shear zone width of 500–2500 m.

(2)  $\theta'$  (first method) and  $\alpha'$  (second method) should be determined with great accuracy, especially for high strains for which a small measurement error in these angles gives a large error in the calculated value of  $\gamma$  (Ramsay & Graham 1970).

(3) The deformation is assumed to have been plane strain, but some flattening component probably exists, because on the western side of the shear zone, in the polyphase Pan-African gneisses, the vertical N-S  $D_2$  folds have been exaggerated during  $D_3$ . In the eastern side of the shear zone, the highest value of  $\theta'$  measured is  $30^\circ$ . If this correctly indicates a shortening component during  $D_3$  of about 8% (Burg & Laurent 1978), then the displacement calculated with the three methods will be overestimated.

(4) In the case of the Abeibara-Rarhous shear zone, use of the second method ( $\alpha'$ ) is very imprecise because of two uncertainties in the value of  $\alpha$ . First,  $\alpha$  is assumed to be the angle between the layering and the shear plane just before the point where the former plane begins to turn towards the latter, so that  $\alpha$  is the highest measured value of  $\alpha'$ . In fact,  $\alpha$  is probably overestimated, and thus  $\gamma$  is also too high, because we cannot map on aerial photographs the precise eastern limit where shear strain begins. Further, the orientation of the granulitic layering 2000 m away from the centre of the shear zone could be in part the result of  $D_3$  folding or of earlier Eburnean folding. Secondly,  $\alpha$  is assumed to be constant along one cross-section but we know that the Eburnean layering may vary in azimuth.

(5) The third method, involving thickness of the mylonitic layering, has some specific limitations inherent in the assumptions made for calculating  $\gamma$ .

(a) The shape, size, and distribution of biotite clusters in undeformed rocks are assumed to be round, constant and homogeneous, respectively. These are good approximations based on observations made on many undeformed rocks and allow us to take a reasonable average value of  $n$ .

(b) The biotite and opaque mineral clusters must have the same rheological properties as the quartz-feldspathic matrix. As the percentage of these clusters in the rock is small (about 5–10%), the difference of plasticity would have important consequences only in the case of hard clusters in a ductile matrix. Neither pressure shadows nor strain heterogeneities are observed around the clusters, so plasticity differences were not important. Actually, the least plastic minerals in the rocks are the zircons and the mesoperthitic feldspars (Boullier 1980). Moreover, as soon as a small grain size is attained by deformation, and if grain boundary sliding is the principal deformation mechanism, ductility contrasts between different minerals should be negligible.

Consequently, it seems that in the case of the Abeibara–Rarhous shear zone and of the shear zones in polyphase gneisses, the first and third methods should give equivalent results, whereas the second method is much less precise because of the irregularity of the planar structures initially. It thus appears reasonable to take the value of half the displacement along the  $D_3$  Abeibara–Rarhous shear zone to be 2 km, as indicated by methods one and three.

## DISCUSSION AND CONCLUSIONS

The dextral sense of shear of the Abeibara–Rarhous shear zone has been demonstrated to be consistent from the map scale to the scale of the quartz lattice. Different methods of strain determination have been used to calculate the displacement along the shear zone, and the average value of displacement is determined to be 4 km.

The measured displacement is low when the total width of the mylonitic zone is considered, but appears reasonable because large extensional or compressional  $D_3$  structures are lacking on the northern termination of the Abeibara–Rarhous shear zone (Fig. 6). We have seen that the western and widest part of the mylonitic zone (5–6 km) corresponds to Pan-African gneisses which have suffered three deformations ( $D_1$ ,  $D_2$  and  $D_3$ ), two of them being mylonitic ( $D_1$  and  $D_3$ ). The parallelism of the older  $D_1$  and  $D_2$  structures with the  $D_3$  shear zone prevent the determination of the amount of strain attributable to each event. Fortunately, however, it is possible to determine  $D_3$  shear strain in the granulitic rocks. Moreover, the map of the northern termination of the Abeibara–Rarhous shear zone (Fig. 6) allows us to affirm that the  $D_3$  shear strain is not greater in the western part of the shear zone than in the eastern part: actually, the northern limit of the granulitic unit is only

slightly displaced and the  $S_3$  trajectories in the pre- $D_3$  granite indicate a displacement of only 1 km. Thus the total amount of movement on the Abeibara–Rarhous shear zone can be estimated to be about 4 km. Consequently, it must be emphasized that the amount of displacement along a shear zone is not necessarily a function of its apparent width on aerial and satellite photographs.

Now, let us consider the regional geological context of the Abeibara–Rarhous shear zone, in the Adrar des Iforas and in the Trans-Saharan Pan-African belt (Cahen & Snelling 1984). We know that the shortening direction is approximately N–S during  $D_1$ , then NNW–SSE to ESE–WNW during  $D_2$ . The  $D_3$  deformation is characterized by N–S to N-20° dextral shear zones or strike-slip faults for which a NE–SW shortening direction is assumed. We think that no gap exists at least between  $D_2$  and  $D_3$  and that the shortening direction rotated continuously.

Ball (1980) described a network of conjugate brittle faults throughout the Hoggar Shield that corresponds to an E–W shortening direction. This event ( $D_4$ ) postdates the  $D_3$  shear zones and is related to the final deformation of the Pan-African mobile belt by the rigid–plastic indentation of the West African Craton (Ball 1980). The shear bands which have been observed in the ultramylonites of the Abeibara–Rarhous shear zone are assumed to represent an intermediate position of the shortening direction between NE–SW ( $D_3$ ) and E–W ( $D_4$ ).

How can such a rotation of the shortening direction be explained in a collisional belt? This rotation does not fit well with a simple E–W collision as proposed by Black *et al.* (1979), Caby (1978), Bayer & Lesquer (1978) and Caby *et al.* (1981). However, it could be explained in a collisional belt with lateral displacement of blocks, as has been proposed for the Alpine System of the Mediterranean Sea (Tapponnier 1977) and for eastern Asia (Peltzer *et al.* 1982), where a 40° rotation is assumed for the Indochina block. Such a model has been proposed by Lesquer & Louis (1982) for the Trans-Saharan Pan-African belt, the initial continental contact having occurred along the Niamey promontory of the West African Craton (Fig. 1) and having produced as a consequence the displacement of the Iforas block NNW along dextral strike-slip shear zones or faults. The displacement could have been as much as 500 km or more along such faults. Such movement is not indicated along the shear zones and faults of the Adrar des Iforas for which strain and displacement data are available (4 and 28 km). Moreover, we have seen that the dextral shear zones postdate the SE–NW to E–W  $D_2$  shortening and are late Pan-African structures. Consequently, the model of Lesquer & Louis (1982) remains speculative. At the moment, no satisfactory answer can be proposed for the rotation of the shortening direction. An oblique collision could be a solution. But more data are needed on paleomagnetism, age and kinematics of the different deformation phases along the belt, and amplitude of displacement along some faults in Algeria and Mali, to refine such a collisional model for the Trans-Saharan Pan-African belt.

**Acknowledgements**—The author is grateful to J. M. Bertrand, A. Pécher and L. I. Wright for fruitful discussions, to anonymous referees for providing useful comments, and to J. Guilbert and P. J. Hudleston for many improvements of the English text. This work has been supported by the C.N.R.S. (France) and by the D.N.G.M. (Mali).

## REFERENCES

- Ashby, M. F. & Verrall, R. A. 1973. Diffusion-accommodated flow and superplasticity. *Acta metall.* **21**, 149–163.
- Ball, E. 1980. An example of very consistent brittle deformation of a wide intracontinental zone: late Pan-African fracture system of the Tuareg and Nigerian shield; structural implications. *Tectonophysics* **61**, 363–379.
- Ball, E. & Caby, R. 1985. Open folding and wrench movements, their relationships with horizontal tectonics in the Pan-African belt of northern Mali. In: *African Geology, Volume in Honour of L. Cahen* (Edited by Klercks, J. & Michot, L.) Musée Royal de l'Afrique centrale, Tervuren, 75–89.
- Bayer, R. & Lesquer, A. 1978. Les anomalies gravimétriques de la bordure orientale du Craton Ouest-Africain: géométrie d'une suture Pan-Africaine. *Bull. Soc. géol. Fr. 7 Sér.* **20**, 863–876.
- Berthé, D., Choukroune, P. & Gapais, D. 1979. Orientations préférentielles du quartz et ortho-gneissification progressive en régime cisailant: l'exemple du cisaillement sud-armoricain. *Bull. Minéral.* **102**, 265–272.
- Bertrand, J. M. L. & Caby, R. 1978. Geodynamic evolution of the Pan-African orogenic belt: a new interpretation of the Hoggar Shield (Algerian Sahara). *Geol. Rdsch.* **67**, 357–388.
- Bertrand, J. M. & Davison, I. 1981. Pan-African granuloid emplacement in the Adrar des Iforas mobile belt (Mali): a Rb/Sr isotope study. *Precambrian Res.* **14**, 333–361.
- Bertrand, J. M., Michard, A., Carpena, J., Boullier, A. M., Dautel, D. & Ploquin, A. 1985. Pan-African granitic and related rocks in the Iforas granulites (Mali). Structure, geochemistry and geochronology. In: *African Geology, Volume in Honour of L. Cahen* (Edited by Klercks, J. & Michot, L.) Musée Royal de l'Afrique centrale, Tervuren, 147–165.
- Black, R., Caby, R., Moussine-Pouchkine, A., Bayer, R., Bertrand, J. M., Boullier, A. M., Fabre, J. & Lesquer, A. 1979. Evidence for late Precambrian plate tectonics in West-Africa. *Nature, Lond.* **278**, 223–227.
- Bouchez, J. L. 1977. Plastic deformation of quartzites at low temperature in an area of natural strain gradient. *Tectonophysics* **39**, 25–50.
- Bouchez, J. L. & Mercier, J. C. 1974. Construction automatique des diagrammes de densité d'orientation. Présentation d'un réseau de comptage. *Sciences de la Terre*, **19**, 57–64.
- Bouchez, J. L., Delvin, P., Mardon, J. P. & Englander, M. 1979. La diffraction neutronique appliquée à l'étude de l'orientation préférentielle de réseau dans les quartzites. *Bull. Minéral.* **102**, 225–231.
- Bouchez, J. L. & Pécher, A. 1981. The Himalayan Main Central Thrust pile and its quartz rich tectonites in central Nepal. *Tectonophysics* **78**, 23–50.
- Bouchez, J. L., Lister, G. S. & Nicolas, A. 1983. Fabric asymmetry and shear sense in movement zones. *Geol. Rdsch.* **72**, 401–419.
- Boullier, A. M. 1979. Charriage et déformations de l'unité granulitique des Iforas au cours de l'orogénèse Pan-Africaine. *Rev. Géogr. phys. Géol. dyn. Paris* **21**, 377–382.
- Boullier, A. M. 1980. A preliminary study on the behaviour of brittle minerals in a ductile matrix: example of zircons and feldspars. *J. Struct. Geol.* **2**, 211–217.
- Boullier, A. M. 1982. Etude structurale du centre de l'Adrar des Iforas (Mali). Mylonites et tectogénèse. Unpublished thèse etat, I.N.P.L., Nancy.
- Boullier, A. M., Davison, I., Bertrand, J. M. & Coward, M. P. 1978. L'unité granulitique des Iforas: une nappe de socle d'âge Pan-Africain précoce. *Bull. Soc. géol. Fr. 7 Sér.* **20**, 877–882.
- Boullier, A. M. & Gueguen, Y. 1975. SP-mylonites: origin of some mylonites by superplastic flow. *Contr. Miner. Petrol.* **50**, 93–104.
- Boullier, A. M. & Bouchez, J. L. 1978. Le quartz en rubans dans les mylonites. *Bull. Soc. géol. Fr. 7 Sér.* **20**, 253–262.
- Burg, J. P. & Laurent, P. 1978. Strain analysis of a shear zone in a granodiorite. *Tectonophysics* **47**, 15–42.
- Caby, R. 1968. Une zone de décrochements à l'échelle de l'Afrique dans le Précambrien de l'Ahaggar occidental. *Bull. Soc. géol. Fr. 7 Sér.* **10**, 577–587.
- Caby, R., Bertrand, J. M. L. & Black, R. 1981. Pan-African ocean closure and continental collision in the Hoggar-Iforas segment, Central Sahara. In: *Precambrian Plate Tectonics* (Edited by Kröner, A.). Elsevier, Amsterdam, 407–434.
- Caby, R. 1978. Paléodynamique d'une marge passive et d'une marge active au Précambrien Supérieur: leur collision dans la chaîne Pan-Africaine du Mali. *Bull. Soc. géol. Fr. 7 Sér.* **20**, 857–862.
- Cahen, L. & Snelling, N. J. 1984. *The Geochronology and Evolution of Africa*. Oxford Science Publications.
- Chinnery, M. A. 1966. Secondary faulting—I. Theoretical aspects and II. Geological aspects. *Can. J. Earth Sci.* **3**, 163–174, 175–190.
- Davison, I. 1980. A tectonic, petrographical and geochronological study of a Pan-African belt in the Adrar des Iforas and Gourma (Mali). Unpublished Ph.D. thesis, University of Leeds and C.G.G. Montpellier.
- Etchecopar, A. 1977. A plane kinematic model of progressive deformation in a polycrystalline aggregate. *Tectonophysics* **39**, 121–142.
- Gapais, D. & White, S. H. 1982. Ductile shear bands in a naturally deformed quartzite. *Textures Microstruct.* **5**, 1–17.
- Garcia Celma, A. 1982. Domainal and fabric heterogeneities in the Cap de Creus quartz mylonites. *J. Struct. Geol.* **4**, 443–455.
- Hobbs, B. E. 1968. Recrystallization of single crystals of quartz. *Tectonophysics* **6**, 353–401.
- Lancelot, J. R., Boullier, A. M., Maluski, H. & Ducrot, J. 1983. Deformation and related radiochronology in a late Pan-African mylonitic shear zone, Adrar des Iforas (Mali). *Contr. Miner. Petrol.* **82**, 312–326.
- Lelubre, M. 1952. Recherches sur la géologie de l'Ahaggar central et occidental (Sahara central). *Bull. Serv. Carte géol. Algérie Série 2*, No. 22, Alger.
- Lesquer, A. & Louis, P. 1982. Anomalies gravimétriques et collision continentale au Précambrien. *Geoexploration* **20**, 275–293.
- Lister, G. S. & Hobbs, B. E. 1980. The simulation of fabric development during plastic deformation and its application to quartzite: the influence of deformation history. *J. Struct. Geol.* **2**, 355–370.
- Lister, G. S. & Snoke, A. W. 1984. S-C Mylonites. *J. Struct. Geol.* **6**, 617–638.
- Marjoribanks, R. W. 1976. The relation between microfabric and strain in a progressively deformed quartzite sequence from Central Australia. *Tectonophysics* **32**, 269–293.
- Molnar, P. & Tapponnier, P. 1975. Cenozoic tectonics of Asia: effects of a continental collision. *Science, Wash.* **189**, 419–426.
- Nicolas, A., Boudier, F. & Boullier, A. M. 1973. Mechanisms of flow in naturally and experimentally deformed peridotites. *Am. J. Sci.* **273**, 853–876.
- Peltzer, G., Tapponnier, P. & Cobbold, P. 1982. Les grands décrochements de l'Est Asiatique, évolution dans le temps et comparaison avec un modèle expérimental. *C. r. hebd. Séanc. Acad. Sci., Paris* **294**, 1341–1348.
- Platt, J. P. & Vissers, R. L. M. 1980. Extensional structures in anisotropic rocks. *J. Struct. Geol.* **2**, 397–410.
- Ramsay, J. G. 1967. *Folding and Fracturing of Rocks*. McGraw-Hill, New York.
- Ramsay, J. G. 1980. Shear-zone geometry: a review. *J. Struct. Geol.* **2**, 83–100.
- Ramsay, J. G. & Graham, R. H. 1970. Strain variations in shear belts. *Can. J. Earth Sci.* **7**, 786–813.
- Schmid, S. M., Casey, M. & Starkey, J. 1981. An illustration of the advantages of a complete texture analysis described by the orientation distribution function (O.D.F.) using quartz pole figure data. *Tectonophysics* **78**, 101–117.
- Simpson, C. & Schmid, S. M. 1983. An evaluation of criteria to deduce the sense of movement in sheared rocks. *Bull. geol. Soc. Am.* **94**, 1281–1288.
- Starkey, J. & Cutforth, C. 1978. A demonstration of the interdependence of the degree of quartz orientation and the quartz content of deformed rocks. *Can. J. Earth Sci.* **15**, 841–847.
- Tapponnier, P. 1977. Evolution tectonique du système alpin en Méditerranée: poinçonnement et écrasement rigide-plastique. *Bull. Soc. géol. Fr. 7 Sér.* **19**, 347–460.
- White, S. H. 1976. The effects of strain on the microstructures, fabrics and deformation mechanisms in quartzites. *Phil. Trans. R. Soc. Lond.* **A283**, 69–86.
- Wilson, C. J. L. 1973. The prograde microfabric in a deformed quartzite sequence, Mount Isa, Australia. *Tectonophysics* **19**, 39–81.
- Wright, L. I. 1979. The pattern of movement and deformation during the Pan-African, in the Adrar des Iforas of Mali. *X Coll. Afr. Geol. Montpellier*, 77.